







## Estimation of Global Solar Radiation Using NNARX Neural Networks Based on the UV Index

### Estimación de la radiación solar global utilizando redes neuronales NNARX basadas en el índice UV

John Barco-Jiménez <sup>1</sup>, Francisco Eraso-Checa <sup>2</sup>, Andrés Pantoja <sup>3</sup>, Eduardo Caicedo-Bravo <sup>4</sup>

Fecha de Recepción: 02 de agosto de 2021

Fecha de Aceptación: 12 de agosto de 2021

**Cómo citar:** Barco-Jiménez., J. Eraso-Checa., F. Pantoja., A. y Caicedo-Bravo., E. (2021). Estimation of Global Solar Radiation Using NNARX Neural Networks Based on the UV Index. *Tecnura*, 25(70), 90-107. <https://doi.org/10.14483/22487638.18638>

## Abstract

**Context:** This work presents different models based on artificial neural networks, among them NNARX, for estimating global solar radiation from UV index measurements. The objective is to determine the efficiency of the models studied to estimate global solar radiation in terms of the coefficient of determination ( $R^2$ ), the root-mean-square error (RMSE), and the mean absolute error (MAE).

**Methodology:** It is divided into four stages: i) conformation of the training dataset (in this case, it uses a training set of 213.019 data collected over five years in the city of Pasto, Colombia, with the Davis Vantage Pro 2.0 station); ii) pre-processing of data to remove erroneous and unusual data; iii) definition of models based on recurrent and conventional artificial neural networks according to an analysis of topologies, e.g. NNFIR and NNARX; iv) training of the models and evaluation of the estimation efficiency through metrics such as  $R^2$ , RMSE, and MAE. To validate the model, a new dataset collected during the last year was used, which was not included in the data training.

**Results:** The global solar radiation estimation models based on NNARX show the best estimation efficiency compared to conventional neural networks. The NNARX221 model has an RMSE of 54,32 and a MAE of 18,06 W/m<sup>2</sup>.

**Conclusions:** NNARX models are highly efficient at estimating global solar radiation, with a coefficient of determination of 0,9697 in the best of cases. The most efficient models are characterized by using two past times and the current UV index instant, and they feed from two past times of their own estimated radiation output. Furthermore, the numerical results show that the contribution of temperature and relative humidity is not relevant to improving the efficiency of the estimation of global solar radiation. These models can be particularly important since they only use measurements made with

<sup>1</sup>Master's degree in Electronics and Computer Engineering, Electronics Engineer. PhD candidate in Electric and Electronics Engineering at Universidad del Valle, San Juan de Pasto, Colombia. Email: [john.barco@correounivalle.edu.co](mailto:john.barco@correounivalle.edu.co).

<sup>2</sup>Master's degree in Engineering, Electronics Engineer. Professor of the Electronics Engineering program of Universidad CESMAG, San Juan de Pasto, Colombia. Email: [feraso@unicesmag.edu.co](mailto:feraso@unicesmag.edu.co).

<sup>3</sup>PhD in Engineering, Master's degree in Electronics and Computer Engineering, Electronics Engineer. Professor of the Department of Electronics Engineering of Universidad de Nariño, San Juan de Pasto, Colombia. Email: [ad\\_pantoja@udenar.edu.co](mailto:ad_pantoja@udenar.edu.co).

<sup>4</sup>PhD in Industrial Informatics, Master's degree in Information Technologies, Electrical Engineer. Professor of the graduate programs in Electrical and Electronics Engineering of Universidad del Valle, Santiago de Cali, Valle, Colombia. Email: [eduardo.caicedo@correounivalle.edu.co](mailto:eduardo.caicedo@correounivalle.edu.co).

UV index sensors, which are less expensive than solar radiation ones.

**Keywords:** recurrent neural network, Davis Vantage PRO 2.0, solar radiation model, solar radiation, UV index.

---

## Resumen

**Contexto:** Este trabajo presenta diferentes modelos basados en redes neuronales artificiales, entre ellas las NNARX, para la estimación de la radiación solar global a partir de mediciones del índice UV. El objetivo es determinar la eficiencia de los modelos estudiados para estimar la radiación solar global en términos del coeficiente de determinación ( $R^2$ ), la raíz del error medio cuadrático (RMSE) y el error absoluto medio (MAE).

**Metodología:** Se divide en cuatro etapas: i) conformación del set de datos de entrenamiento (en este caso se utiliza un set de entrenamiento de 213.019 datos recolectados durante 5 años en la ciudad de Pasto, Colombia, con la estación Davis Vantage Pro 2.0); ii) pre-procesamiento de los datos para remover datos erróneos e inusuales; iii) definición de modelos basados en redes neuronales artificiales recurrentes y convencionales basándose en un análisis de topologías, *e.g.* NNFIR y NNARX; iv) entrenamiento de los modelos y evaluación de la eficiencia de la estimación por medio de métricas como  $R^2$ , RMSE y MAE. Para validar el modelo se utilizaron datos recolectados durante el último año, los cuales no se incluyeron en el entrenamiento.

**Resultados:** Los modelos de estimación de radiación solar global basados en NNARX presentan la mejor eficiencia en la estimación en comparación con redes neuronales convencionales. El modelo NNARX221 presenta un RMSE de 54,32 y un MAE de 18,06 W/m<sup>2</sup>.

**Conclusiones:** Los modelos NNARX tienen una gran eficiencia para estimar la radiación solar global, en el mejor de los casos con un coeficiente de determinación de 0,9697. Los modelos más eficientes se caracterizan por utilizar dos instantes pasados y el instante actual de índice UV y realimentar dos instantes pasados de su propia salida de radiación estimada. Además, los resultados numéricos muestran que la contribución de la temperatura y humedad relativa no es relevante para mejorar la eficiencia de la estimación de la radiación solar global. Estos modelos pueden ser particularmente importantes dado que solamente utilizan mediciones realizadas con sensores de índice UV que son menos costosos que los sensores de radiación solar.

**Palabras clave:** redes neuronales recurrentes, Davis Vantage PRO 2.0, modelo de radiación solar, índice UV.

---

## Table of Contents

	<b>Page</b>
<b>Introduction</b>	<b>92</b>
<b>Methodology</b>	<b>93</b>
Solar radiation . . . . .	93
UV index . . . . .	94
Methodological process . . . . .	95
Estimation models based on ANNs . . . . .	97

<b>Results</b>	<b>99</b>
Meteorological station and data set . . . . .	99
Numerical results . . . . .	100
<b>Conclusions</b>	<b>104</b>
<b>Acknowledgements</b>	<b>104</b>
<b>References</b>	<b>104</b>

## INTRODUCTION

Solar radiation data have become important due to the increase in the use of solar energy. In general, solar radiation data are obtained from long-term monitoring stations, and they are used for photovoltaic applications or thermal heating, cooling, or drying systems.

To design an accurate photovoltaic system according to a specific zone, it is necessary to perform an irradiance study using radiation sensors such as pyranometers, pyrhemometers, or sunphotometers. However, this kind of sensors are usually expensive, especially in cases where a large number of them is necessary.

The literature has several models and studies used to detect radiation at lower costs ([Cruz-Colón et al., 2012](#)). [Chacón et al., 2008](#) and [Ortiz & Peng 2005](#) developed a low cost irradiance sensor that describes the electric behavior of a photovoltaic module using an exponential model applied to a solar cell. The maximum error between the estimated and measured irradiance was 1,11 %. [Abe et al., 2020](#) proposed a sensor based on a phototransistor. They used the arithmetic mean for the ungrouping data method ([Viljoen & Merwe, 2000](#)). The results of the simulation showed a determination coefficient ( $R^2$ ) of 0,99099 with respect to the pyranometer. [Mancilla-David et al., 2014](#) introduced a solar irradiance sensor using a photovoltaic cell, a temperature detector, and a low-cost microcontroller programmed with an artificial neural network to determine the irradiance. Under ordinary operating conditions, simulation and experimental results showed that these methods can obtain an accurate estimation. However, it is difficult to collect complete data to train these soft sensors. In addition, as time passes, a solar cell will change its electrical characteristics.

[Sayago et al., 2011](#), [Ruiz-Cárdenas et al., 2016](#), and [Moreno et al., 2012](#) used neural network models capable of estimating solar radiation through meteorological variables such as temperature, relative humidity, wind speed, and rainfall. The results show determination coefficients between 0,80 and 0,86 and root mean square errors values (RMSE) between 25 % and 48 %. [Khan et al., 2013](#), [Capizzi et al., 2012](#), and [Aliberti et al., 2021](#) explored models to estimate global solar radiation based on artificial neural networks (ANN), e.g. second-generation Wavelets with ANN, Long Short-Term Memory (LSTM), Feed-Forward Neural Networks (FFNN). The results show that the best models

reached a correlation coefficient of 0,98 for Wavelet and ANN. The model based on LSTM obtained an RMSE equal to 113 Wh/m<sup>2</sup> and a determination coefficient of 0,9744. [Hernández-Mora et al., 2013](#) developed a statistical methodology to determine solar irradiance and the ambient temperature from real measurement data, collected every hour from six in the morning to six in the afternoon. The Anderson-Darling test ([Anderson & Darling, 1952](#), [Torres, 2002](#)) was applied to these data, thus achieving a correlation coefficient higher than 0,96 for each hour. Despite being a reliable model, it is necessary to have a database of at least five years. [Obando et al., 2019](#) presented a literature review of ANN models for solar radiation estimation. It analyses different ANN structures under several performance criteria, providing a decision methodology to evaluate ANN models for solar radiation prediction.

[Korachagaon et al., 2015](#) proposed several polynomial models to estimate global solar radiation using variables such as, ratio of duration of sunshine to maximum sunshine hours, mean temperature, and mean relative humidity. The models allow estimating radiation at any location of the earth's surface. Some results showed that the least RMSE is within 0,185, and a correlation coefficient of the measured and estimated global solar radiation was found to be 0,52494. Likewise, [Eraso-Checa et al., 2018](#) proposed a polynomial to estimate global radiation from the UV index, which is valid for Pasto, Colombia. The results showed a correlation factor of 0,9642, and the RMSE is 30,90, which is acceptable for mid-range and low-end measurement devices.

The main contribution of this paper is that it explores the relationship between the UV index and solar radiation. The responses of these variables have a similar behavior, and the spectral response curves denote similar characteristics. This work uses an ANN trained with radiation and UV index data, and it determines the radiation based on UV index measurement and time. This estimation model becomes relevant because UV sensors are cheaper than radiation sensors, and generally they occupy less space.

This paper is organized as follows: first, it presents the theoretical aspects related to the UV index and irradiance; second, the methodology is presented and described; third, all recurrent neural networks based on NNARX models are presented; and finally, the results and conclusions are presented.

## METHODOLOGY

### Solar radiation

The Sun is the Earth's main energy source. This star emits electromagnetic radiation of different frequency and wavelength in the electromagnetic spectrum. Solar radiation in the atmosphere has a wavelength between 150 nm and 4.000 nm, where 7% corresponds to ultraviolet radiation, 47% to visible radiation, and 46% to infrared radiation ([Eraso-Checa et al., 2017](#), [Würfel, 2009](#)). However, the wavelength that reaches the Earth's surface is attenuated to a range between 380 nm and 780

nm (Narváez & Hernández, 2013) due to absorption, reflection, and scattering phenomena. This also means that the global radiation on the surface is composed of beam, diffuse, and reflected radiation (Jäger *et al.*, 2014). Another parameter that attenuates solar radiation is the optical air mass, which is the path length that sunlight follows through the atmosphere (Jäger *et al.*, 2014).

Figure 1 shows the power received per unit surface exposed to radiation for each wavelength at the outer side of the Earth's atmosphere. It shows that the visible part of the spectrum has the large area between 400 nm and 700 nm, with a spectral irradiance peak around 2.000 W/m<sup>2</sup>.nm. Ultraviolet (UV) light occupies the high energetic part of the spectrum.

The integration of spectral irradiance over wavelength corresponds to the irradiance, which is a power per unit area (W/m<sup>2</sup> or joules/m<sup>2</sup>sec). This is a magnitude scale that includes the complete wavelength information. Radiation measuring equipment gives the solar radiation response as irradiance (W/m<sup>2</sup>).

## UV index

UV radiation is just a part of the solar spectrum at high frequencies (>10<sup>16</sup> Hz). This means that it is very energetic and can ionize atoms by electrically charging them (Casal, 2010). Photon energy ranges from 3,2 eV up to 1,2x10<sup>3</sup> eV (Bohorquez-Ballén & Pérez-Mogollón, 2007). UV radiation allows human beings to assimilate vitamin D and, in plants, it makes photosynthesis possible. However, it also has negative effects if there is prolonged exposure, especially in human health (it breaks biological molecules, damages the eyes and skin, it causes cancer, etc.) (Bohorquez-Ballén & Pérez-Mogollón, 2007).

UV radiation is divided into three regions (Ryer, 1988):

- *UV-A (315-400 nm)*: It is the least harmful to human beings, and its intensity reaches the terrestrial surface.
- *UV-B (280-315 nm)*: It is toxic to life and can destroy it. Ozone absorbs this energy (approximately 90 %) and prevents it from reaching the Earth (Casal, 2010).
- *UV-C (100-280 nm)*: Its collision with oxygen atoms causes ozone generation, and it does not reach the Earth. This radiation would destroy life.

According to Lucas *et al.*, 2006, ambient UV radiation can be measured using a representation of the wavelength variation in the production of skin erythema. The UV index is an instance of this representation (the other are SED and MED). It is defined as the time-weighted average effective UV irradiance multiplied by 40, and it is expressed as power per unit area (W/m<sup>2</sup>).

Figure 2 shows the behavior of both spectral irradiance and the erythemal action spectrum in the UV region.

The UV index is categorized as shown in Table 1, and the values range from 0 on. The higher the index value, the greater potential damage to the skin in the less time.

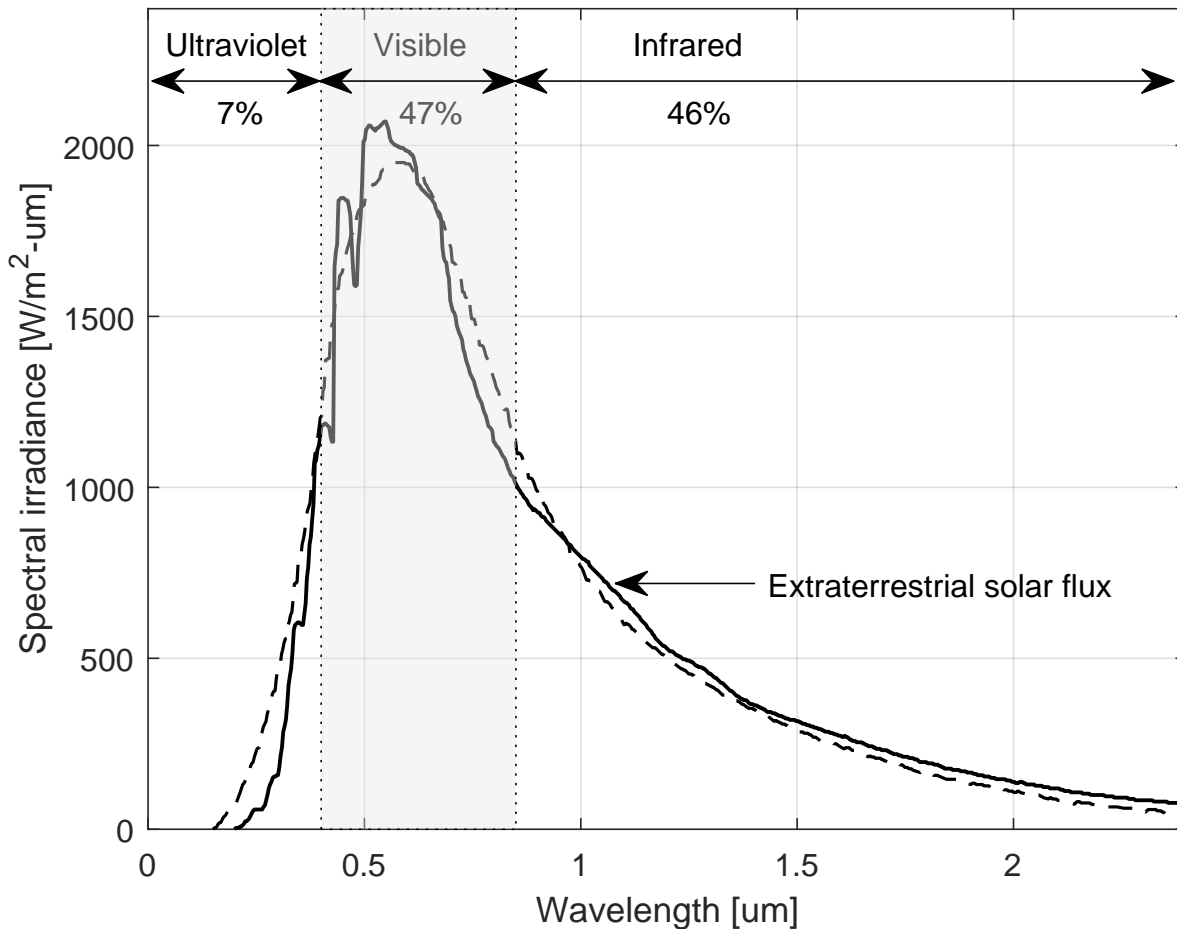


**Figure 1.** Extra-terrestrial solar spectrum

**Source:** (Würfel, 2009).

## Methodological process

To develop and validate the estimation model, a methodological process was carried out, which was adapted from Eraso-Checa *et al.*, 2018. In this case, the methodology used is composed of a typical process that increases estimation reliability. In Figure 3, the methodological process is shown.

A set of climatic variables (UV index, temperature, humidity, and solar radiation) was extracted from the Davis Vantage PRO station. In this case, the dataset is made up of approximately 305.000 data for each variable from 2013 to 2018. Since the first data are raw, it was necessary to remove spurious and erroneous data using an inspection algorithm. This process removes not-a-number data, data equal to infinity, and unusual data such as out-of-range values that are physically impossible to reach. Finally, a training dataset of 213.019 data and a validation dataset of 91.696 were obtained.

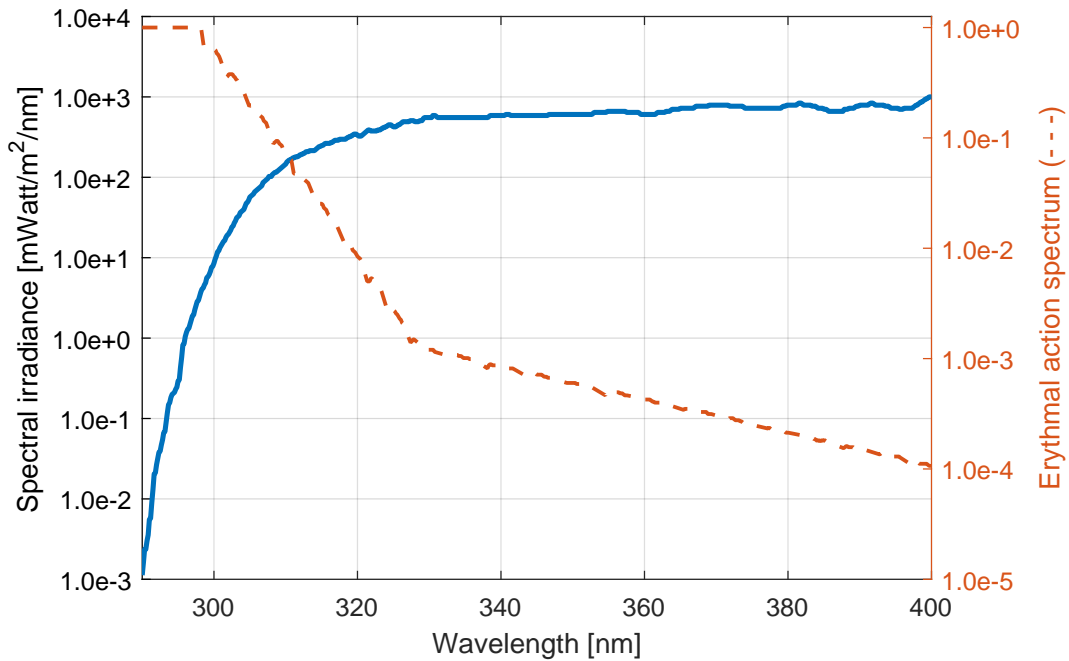


**Figure 2.** UV spectral irradiance and erythemal action spectrum

Source: [National Services Centre \(n.d.\)](#).

**Table 1.** UV index categorization

UV Index	Danger Category
0-2	Low
3-5	Moderate
6-7	High
8-10	Very High
11+	Extreme

Source: [National Services Centre \(n.d.\)](#).

After that, solar radiation was estimated with following steps: first, the estimation model based on neural networks (NN) was defined, considering estimation structures and inputs; secondly, the structure was trained using the dataset; then, there was an evaluation process using the validation dataset, which calculated some predefined metrics such as mean absolute error (MAE), root mean square error (RMSE), and the coefficient of determination ( $R^2$ ).

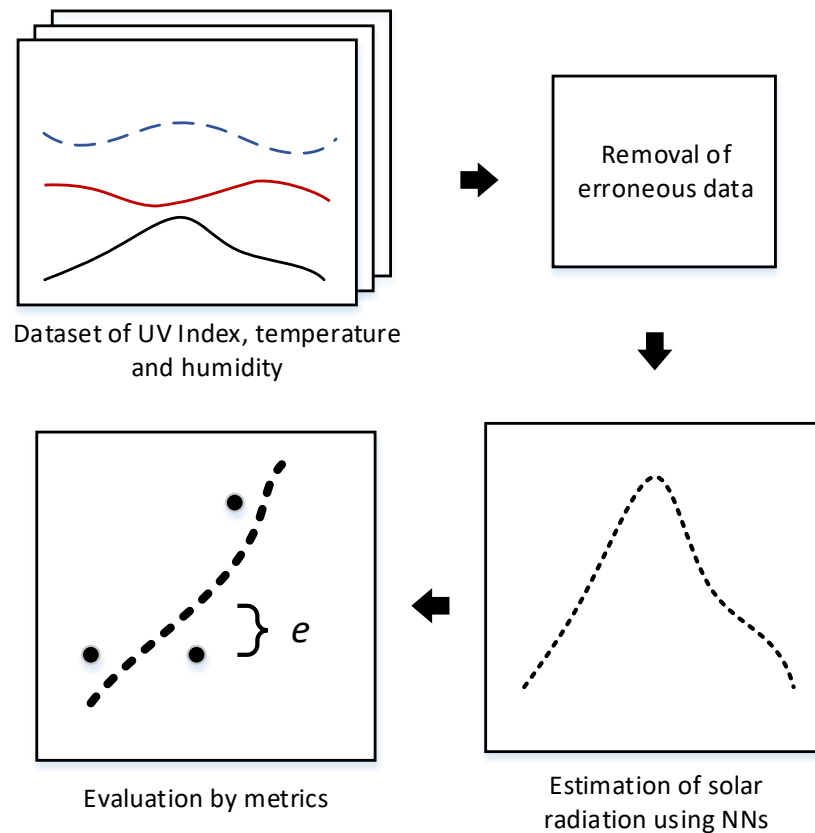


**Figure 3.** Methodological process

Source: Authors.

### Estimation models based on ANNs

Different nonlinear models based on ANNs were used to estimate solar radiation. Mainly, two different ANN structures were used to model the estimators: Neural Network Finite Impulse Response (NNFIR) structure and Neural Network Autoregressive with Exogenous Input (NNARX).

NNFIR is a simple model estimator fed with external excitations to make a prediction. Figure 4 shows, on the left side, a NNFIR that does not have feedback. NNARX is a recurrent neural network. On the right side of Figure 4, the network uses external excitations and past instants to make a prediction.

As shown in Figure 4, the NNFIR and NNARX models are fed with past instants of one or more inputs  $(u_1(\cdot), \dots, u_j(\cdot))$ , and past instants of the estimated output  $(\hat{y}(\cdot))$  in case of the NNARX structure. For more details on NNARX and NNFIR structures, see their description in the referenced literature (Norgaard *et al.*, 2000).



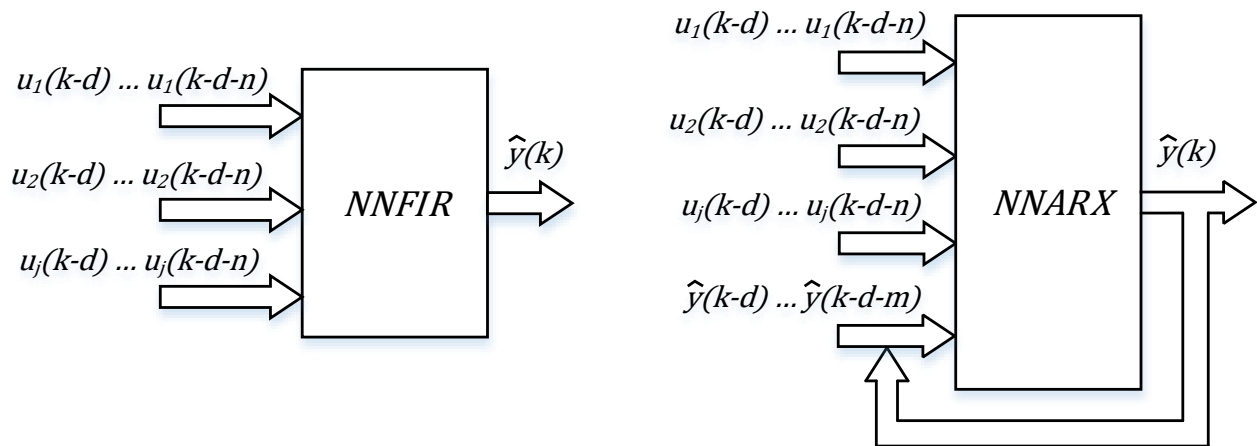


**Figure 4.** NNFIR and NNARX structures

Source: Authors.

In addition, this paper proposes to use the temperature as part of the estimator, aiming to compensate the lack of information of the reduced band in the UV index sensor. In that way, it is possible to quantify the contribution of the temperature in the estimation of solar radiation. To differentiate the models, models that use UV index and/or estimated radiation are denoted with *a* at the end, and the estimation models that use temperature in addition to the UV index and/or estimated radiation are denoted with *b* at the end. The definitions of these models are shown below, and they are summarized in Table 2.

**Table 2.** Mathematical definition of the NNFIR and NNARX models

Model	Mathematical definition
NNFIRa	$R(k)=f(\text{UV}(k))$
NNFIRb	$R(k)=f(\text{UV}(k),T(k))$
NNARX111a	$R(k)=f(R(k-1), \text{UV}(k), \text{UV}(k-1))$
NNARX111b	$R(k)=f(R(k-1), \text{UV}(k), \text{UV}(k-1), T(k), T(k-1))$
NNARX211a	$R(k)=f(R(k-1), R(k-2), \text{UV}(k), \text{UV}(k-1))$
NNARX211b	$R(k)=f(R(k-1), R(k-2), \text{UV}(k), \text{UV}(k-1), T(k), T(k-1))$
NNARX221a	$R(k)=f(R(k-1), R(k-2), \text{UV}(k), \text{UV}(k-1), \text{UV}(k-2))$
NNARX221b	$R(k)=f(R(k-1), R(k-2), \text{UV}(k), \text{UV}(k-1), \text{UV}(k-2), T(k), T(k-1), T(k-2))$

Source: Authors.

$R(\cdot)$  is the global solar radiation,  $UV(\cdot)$  is the UV index,  $T(\cdot)$  is the ambient temperature, and  $k$  is the time instant. NNFIR and NNARX structures are configured as follows: one hidden layer with 20 neurons, sigmoidal activation function, and Bayesian Regularization as the training algorithm.

## RESULTS

In this section, the first part describes the station that collected the raw data. The second one describes the training and validation processes, and then the estimation results are presented by figures and tables with the evaluation metrics.

### Meteorological station and data set

Solar radiation, the UV index, temperature, and humidity data were collected from November 2013 to December 2018 using the DAVIS Vantage Pro 2.0 meteorological station. This equipment uses the 6450 solar radiation sensor (Davis Instruments, 2014a) and the 6490 UV sensor that measures the global solar UV index (Davis Instruments, 2014b).

After applying the methodological process to 305.172 data, a training dataset of 213.019 elements and a validation set of 91.696 data for each variable (30% of total data) were obtained. There were 457 spurious and erroneous data, as shown in Figure 5.

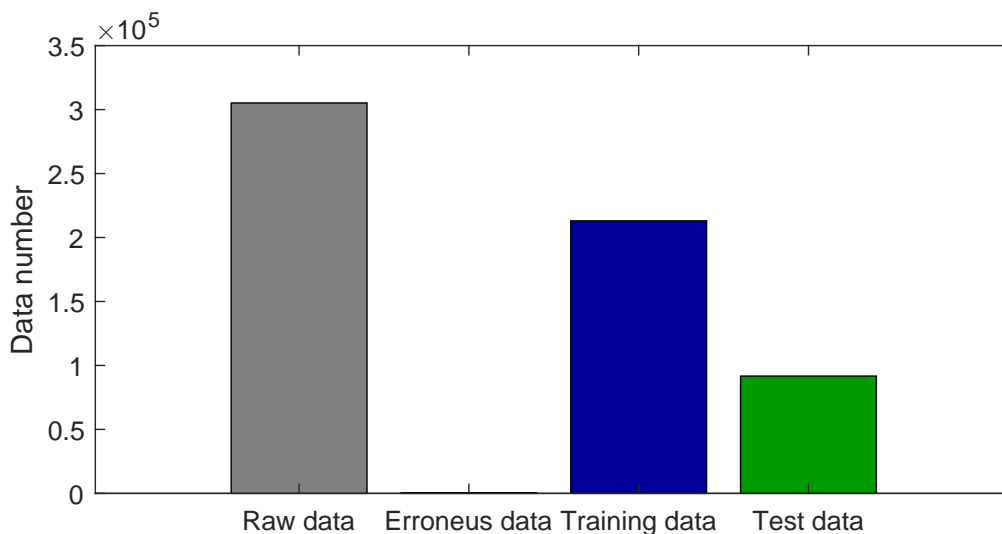


**Figure 5.** Use of data in the solar radiation estimation process

**Source:** Authors.

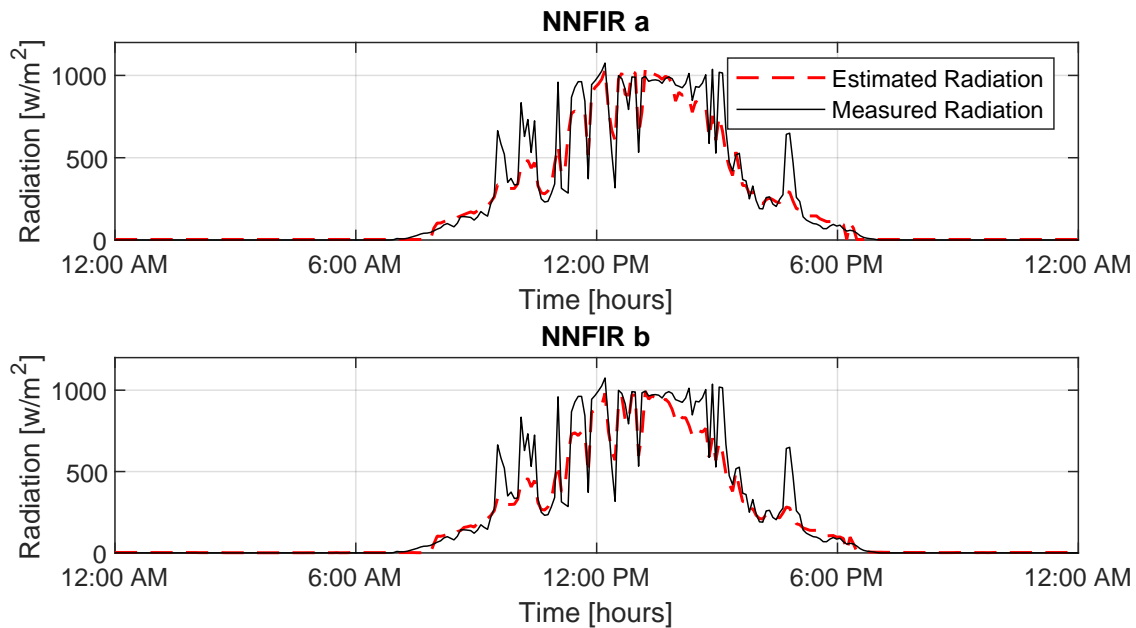


**Figure 6.** Solar radiation estimation using NNFIR1 and NNFIR2 structures

**Source:** Authors.

## Numerical results

The NN MATLAB toolbox was used to train the eight proposed estimation models. Each model was trained using its corresponding dataset (inputs, outputs, and validation dataset).

The following Figures show the solar radiation estimation results using a random day from the validation data set.

As shown in Figure 6, the radiation estimation with the NNFIRa and NNFIRb structures was able to follow the general behavior of the measured radiation. However, the error increases due to instant radiation changes. These models have an estimation error of  $\pm 38.80 \frac{W}{m^2}$  and  $\pm 42.71 \frac{W}{m^2}$  respectively.

The NNARX111a and NNARX111b structures improve the estimation of solar radiation reducing the error to  $\pm 26.60 \frac{W}{m^2}$  and  $\pm 28.61 \frac{W}{m^2}$ , respectively (Figure 7). This optimization occurs because these structures make a prediction using past and present data. Therefore, they have a measurement radiation rate that is used to predict the next radiation value.

Figures 8 and 9 show the NNARX211a, NNARX211b, NNARX221a, and NNARX221b structures. These kind of structures reduce the error between  $\pm 26.27 \frac{W}{m^2}$  and  $\pm 24.53 \frac{W}{m^2}$ . This is possible because the network makes a prediction from two past instants. In the same way, predictions with structures that include more than two past instants were developed. Nevertheless, the error does not reduce its value significantly.

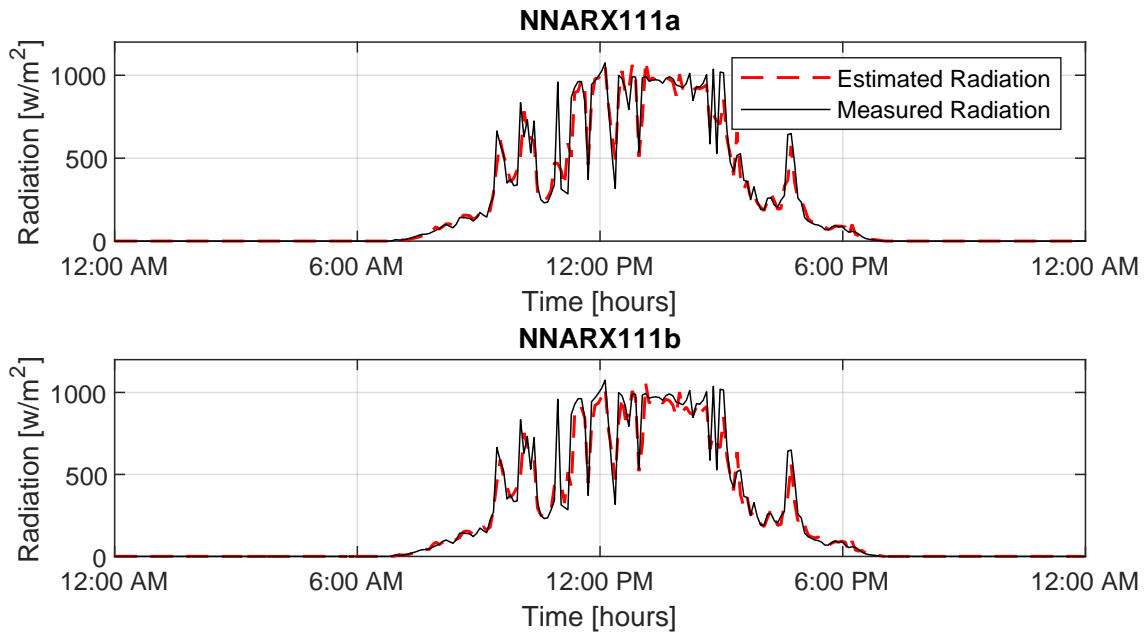


**Figure 7.** Solar radiation estimation using NNARX111a and NNARX111b structures

**Source:** Authors.

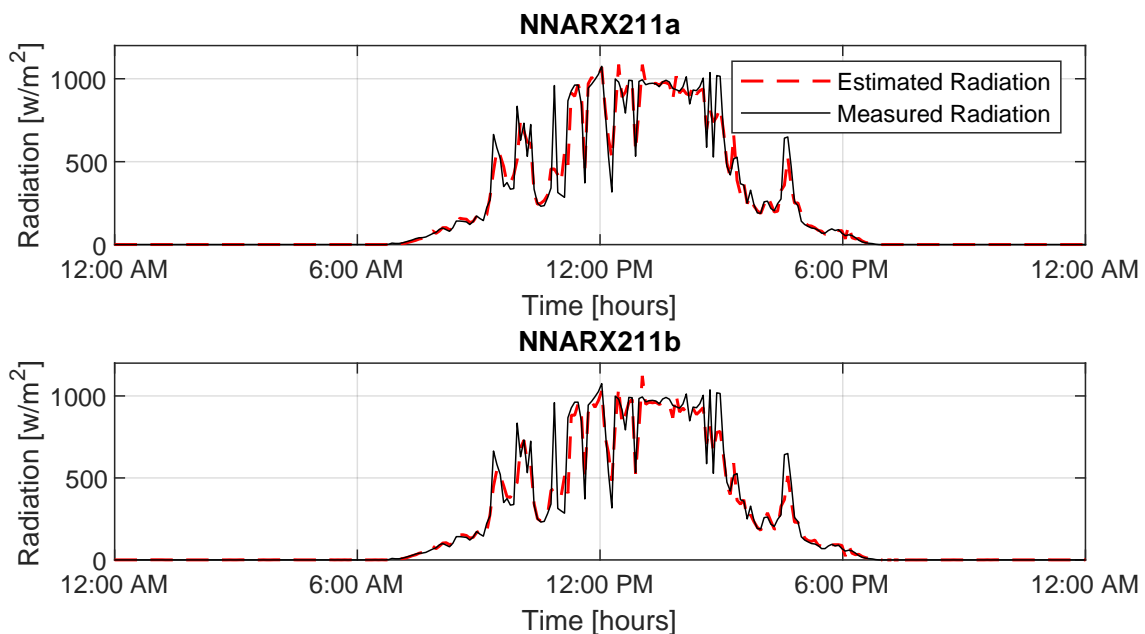


**Figure 8.** Solar radiation estimation using NNARX211a and NNARX211b structures

**Source:** Authors.

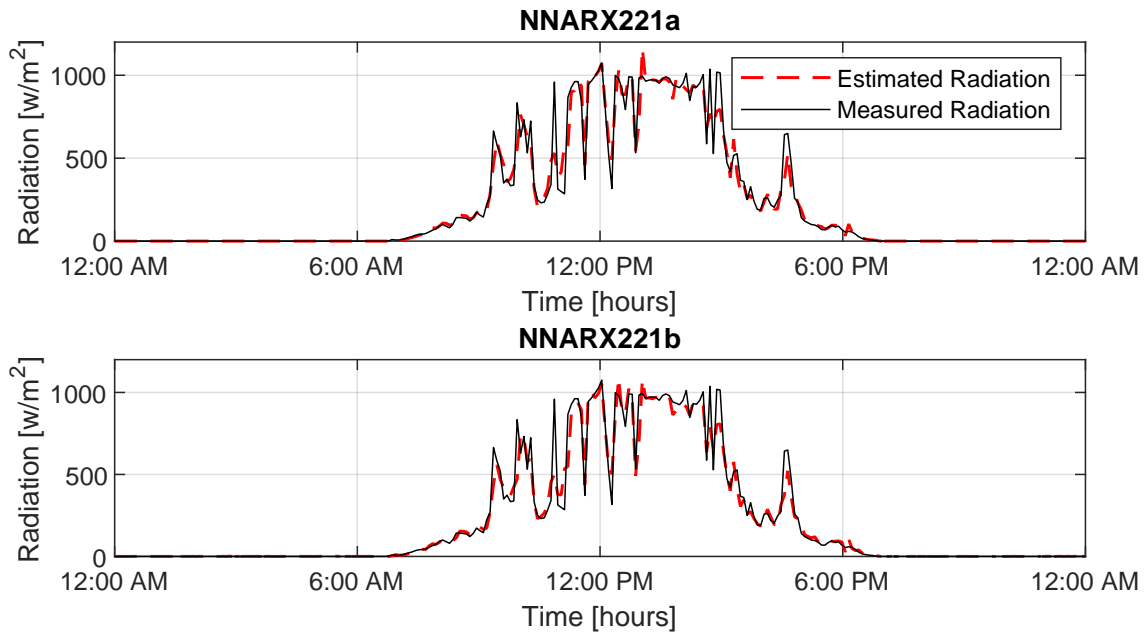


**Figure 9.** Solar radiation estimation using NNARX221a and NNARX221b structures

**Source:** Authors.

From Figures 7-9, it can be noticed that the differences between type *a* and *b* models are not significant. Despite this, type *b* models use other variables (temperature, humidity) to complement the estimation in contrast with type *a* models, which only use the input variable and the past instants. These additional variables do not significantly reduce the error. In contrast, the error increases in some cases.

According to the numerical results presented in Table 3, considering the validation data set (91.696 elements), type *a* models have a similar behavior to type *b* ones. Type *b* models have a smaller RMSE and a bigger  $R^2$  coefficient in comparison with type *a* models. In contrast, type *a* models have a smaller MAE than type *b* models. However, the differences between models *a* and *b* are not significant.

Also, NNARX221a and NNARX221b have the best performance in terms of RMSE, MAE, and  $R^2$  compared to other estimation models.

As seen in the Figure 10 and Table 3, the differences between estimation structures NNARX221a and NNARX221b are not significant. Hence, the contribution of the auxiliary variables (temperature and humidity) in the estimation of solar radiation is not relevant. In this sense, the NNARX221a model has the best performance (based on  $R^2$ ) only using past and present instants of solar radiation and the UV index.

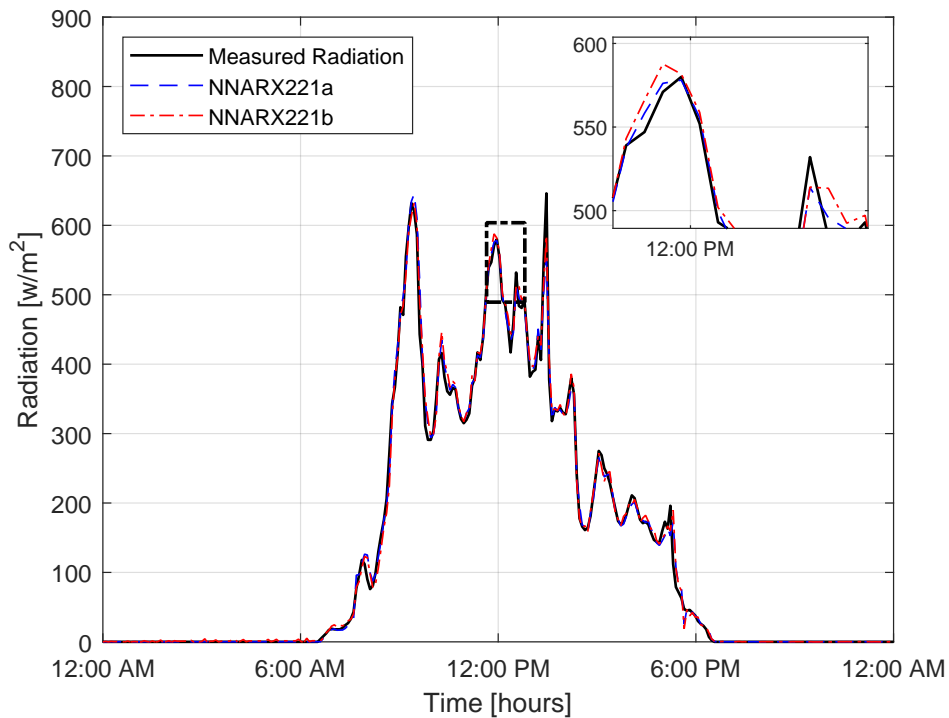


**Figure 10.** Comparison between estimation structures NNARX221a and NNARX221b for a random day  
**Source:** Authors.

**Table 3.** Numerical results of estimation models for the validation dataset

Structure/Metric	RMSE	MAE	R <sup>2</sup>
NNFIRa	87,855	42,526	0,92294
NNFIRb	86,863	41,301	0,92489
NNARX111a	55,835	18,624	0,96805
NNARX111b	55,532	18,643	0,96838
NNARX211a	55,066	18,314	0,96895
NNARX211b	54,809	18,347	0,96925
NNARX221a	54,710	17,905	0,96927
NNARX221b	54,321	18,069	0,96971

**Source:** Authors.

## CONCLUSIONS

This similarity in graphical patterns between the UV index information recorded with the 6490 Davis sensor and the solar radiation data recorded with the 6450 Davis sensor allow estimating solar radiation based on UV index. For this process, there were two NNFIR and eight NNARX-trained structures. The best performance corresponds to a NNARX221 structure that makes a prediction using two past instants that include the UV index and its own outputs. It shows a determination coefficient of 0,9697, a RMSE equal to 54,32, and a MAE of 18,06 W/m<sup>2</sup>. Because of that, the use of this structure allows the determination of solar radiation in an accurate way using the UV index.

The numerical results show that the contribution of the auxiliary variables (temperature and humidity) in the estimation of solar radiation is not relevant. The best estimations are made only using past and present instants of solar radiation and the UV index. This is particularly important since UV index measurement equipment usually has a lower cost than global radiation ones.

For future work, it could be interesting to test other prediction techniques based on artificial intelligence, such as random forests, decision trees, and short-term memories, among others. This methodology and models can be generalized to be used with other variables or time series.

## ACKNOWLEDGEMENTS

This work was supported by the Research Department of Universidad CESMAG in Colombia. Also, the authors gratefully acknowledge the financial support provided by the Colombia Scientific Program within the framework of call named *Ecosistema Científico*, contract No. FP44842- 218-2018, and Fundación CEIBA, contract No. 87067512.

## REFERENCES

- [Abe *et al.*, 2020] Abe, C. F., Dias, J. B., Notton, G., & Faggianelli, G. A. (2020). Experimental application of methods to compute solar irradiance and cell temperature of photovoltaic modules. *Sensors (Switzerland)*, 20(9), 2940. <https://doi.org/10.3390/s20092490> ↑See page 92
- [Aliberti *et al.*, 2021] Aliberti, A., Fucini, D., Bottaccioli, L., Macii, E., Acquaviva, A., & Patti, E. (2021). Comparative analysis of neural networks techniques to forecast Global Horizontal Irradiance. *IEEE Access*, 9, 122829-122846. <https://doi.org/10.1109/ACCESS.2021.3110167> ↑See page 92
- [Anderson & Darling, 1952] Anderson, T. W., & Darling, D. A. (1952). Asymptotic theory of certain "Goodness of fit" criteria based on stochastic processes. *Annals of Mathematical Statistics*, 23(2), 193-212. <https://doi.org/10.1214/aoms/1177729437> ↑See page 93

- [Bohorquez-Ballén & Pérez-Mogollón, 2007] Bohorquez-Ballén, J., & Pérez-Mogollón, J. F. (2007). Radiación Ultravioleta. *Ciencia y Tecnología Para La Salud Visual y Ocular*, 5(9), 97-104. <https://doi.org/10.19052/sv.1520> ↑See page 94
- [Capizzi *et al.*, 2012] Capizzi, G., Napoli, C., & Bonanno, F. (2012). Innovative second-generation wavelets construction with recurrent neural networks for solar radiation forecasting. *IEEE Transactions on Neural Networks and Learning Systems*, 23(11), 1805-1815. <https://doi.org/10.1109/TNNLS.2012.2216546> ↑See page 92
- [Casal, 2010] Casal, C. (2010). *Caracterización de la radiación ultravioleta en la provincia de Huelva e incidencia en la productividad y el valor biotecnológico de cultivos de interés comercial*. Departamento de Química y CCMM, Universidad de Huelva. <http://rabida.uhu.es/dspace/bitstream/handle/10272/2713/b15236572.pdf?sequence=1> ↑See page 94
- [Chacón *et al.*, 2008] Chacón, C. A., Cely, O. E., & Guerrero, F. (2008). Diseño y construcción de un medidor de radiación solar. *Tecnura*, 12(23), 13-23. <https://www.redalyc.org/articulo.oa?id=257020605003> ↑See page 92
- [Cruz-Colón *et al.*, 2012] Cruz-Colón, J., Martínez-Mitjans, L., & Ortiz-Rivera, E. I. (2012, June 3-8). *Design of a low cost irradiance meter using a photovoltaic panel* [Conference presentation]. 38th IEEE Photovoltaic Specialists Conference (PVSC), Austin, TX, USA. <https://doi.org/10.1109/PVSC.2012.6318195> ↑See page 92
- [Eraso-Checa *et al.*, 2017] Eraso-Checa, F., Barco-Jiménez, J., Escobar, D., Insuasty, S. (2017). *Energía Fotovoltaica: Modelos y respuestas a condiciones meteorológicas*. Institución Universitaria CESMAG. <https://doi.org/10.15658/CESMAG17.010807> ↑See page 93
- [Eraso-Checa *et al.*, 2018] Eraso-Checa, F., Jiménez, J. B., Escobar, D., & Insuasty, S. (2018, September 18-21). *Global radiation estimation using a polynomial function on UV index* [Conference presentation]. 2018 IEEE PES Transmission & Distribution Conference and Exhibition - Latin America (T&D-LA), Lima Perú. <https://doi.org/10.1109/TDC-LA.2018.8511791> ↑See page 93, 95
- [Hernández-Mora *et al.*, 2013] Hernández-Mora, J., Trujillo-Rodríguez, C., & Vallejo-Lozada, W. (2013). Modelamiento de la irradiancia y la temperatura ambiente utilizando funciones de probabilidad. *Revista Tecnura*, 18(39), 128-137. <https://doi.org/2014.1.a09> ↑See page 93
- [Davis Instruments, 2014a] Davis Instruments (2014a). *6450 solar sensor datasheet*. Davis Instruments. ↑See page 99
- [Davis Instruments, 2014b] Davis Instruments (2014b). *6490 UV sensor datasheet*. Davis Instruments. ↑See page 99



- [Jägner *et al.*, 2014] Jägner, K., Olindo I., Smets, A., Van-SWaaij, R., & Zeman, M. (2014). *Solar Energy: Fundamental, technology and systems*. Delft University of Technology. ↑See page 94
- [Kamali *et al.*, 2006] Kamali, G. A., Moradi, I., & Khalili, A. (2006). Estimating solar radiation on tilted surfaces with various orientations: a study case in Karaj (Iran). *Theoretical and Applied Climatology*, 84, 235-241. <https://doi.org/10.1007/s00704-005-0171-y> ↑See page
- [Khan *et al.*, 2013] Khan, M. A., Huque, S., & Mohammad, A. (2013, February 13-15). *A neural network model for estimating global solar radiation on horizontal surface* [Conference presentation]. 2013 International Conference on Electrical Information and Communication Technology, (EICT), Khulna, Bangladesh. <https://doi.org/10.1109/EICT.2014.6777857> ↑See page 92
- [Korachagaon *et al.*, 2015] Korachagaon, I., Mudgal, D. N., Kottur, R. M., Patil, S. K., & Bapat, V. N. (2015, January 9-10). *Global Solar Radiation Estimation Model with Two Parameters and its ANN validation* [Conference presentation]. 2015 IEEE 9th International Conference on Intelligent Systems and Control (ISCO), Coimbatore, India. <https://doi.org/10.1109/ISCO.2015.7282286> ↑See page 93
- [Lucas *et al.*, 2006] Lucas, R., McMichael, T., Smith, W., & Armstrong, B. (2006). *Solar Ultraviolet Radiation: Global burden of disease from ultraviolet radiation*. World Health Organization. ↑See page 94
- [Mancilla-David *et al.*, 2014] Mancilla-David, F., Riganti-Fulginei, F., & Laudani, A. (2014). A neural network-based low-cost solar irradiance sensor. *IEEE Transactions on Instrumentation and Measurement*, 63(3), 583-591. <https://doi.org/10.1109/TIM.2013.2282005> ↑See page 92
- [Moreno *et al.*, 2012] Moreno, C. M., Pedraza, L. F., & Rivas, E. (2012). Predicción de la demanda de energía eléctrica basado en análisis Wavelet y un modelo neuronal auto-regresivo no lineal NAR. *Tecnura*, 16(Special Issue), 86-99. <https://doi.org/10.14483/22487638.6816> ↑See page 92
- [Narváez & Hernández, 2013] Narváez, J. A., & Hernández, R. (2013). *Determinación del modelo técnico adecuado para el aprovechamiento de la energía fotovoltaica en Pasto*. Institución Universitaria CESMAG. ↑See page 94
- [National Services Centre (n.d.)] National Services Centre (n.d.). *Climate Prediction Center: UV index information*. [https://www.cpc.ncep.noaa.gov/products/stratosphere/uv\\_index/uv\\_current.shtml](https://www.cpc.ncep.noaa.gov/products/stratosphere/uv_index/uv_current.shtml) ↑See page 96
- [Norgaard *et al.*, 2000] Norgaard, M., Ravn, O., Poulsen, N. K., & Hansen, L. K. (2000). *Neural Networks for Modelling and Control of Dynamic Systems*. Springer-Verlag. <https://doi.org/10.1007/978-1-4471-0453-7> ↑See page 97

- [Obando *et al.*, 2019] Obando, E. D., Carvajal, S. X., & Pineda, J. (2019). Solar Radiation Prediction Using Machine Learning Techniques: A Review. *IEEE Latin America Transactions*, 17(4), 684-697. <https://doi.org/10.1109/TLA.2019.8891934> ↑See page 93
- [Ortiz & Peng 2005] Ortiz, E. I., & Peng, F. Z. (2005). *Analytical Model for a Photovoltaic Module Using the Electrical Characteristics provided by the Manufacturer Data Sheet* [Conference presentation]. 36th IEEE Power Electronics Specialists Conference, Dresden, Gemany. <https://doi.org/10.1109/PESC.2005.1581920> ↑See page 92
- [Ruiz-Cárdenas *et al.*, 2016] Ruiz-Cárdenas, L. C., Amaya-Hurtado, D., & Jiménez-Moreno, R. (2016). Predicción de radiación solar mediante deep belief network. *Tecnura*, 20(47), 39-48. <https://doi.org/10.14483/udistrital.jour.tecnura.2016.1.a03> ↑See page 92
- [Ryer, 1988] Ryer, A. (1988). *Light measurement handbook*. Technical Publications Department, International Light, Inc. ↑See page 94
- [Sayago *et al.*, 2011] Sayago, S., Bocco, M., Ovando, G., & Willington, E. (2011). Radiación solar horaria: modelos de estimación a partir de variables meteorológicas básicas. *Avances En Energías Renovables y Medio Ambiente*, 15, 102488. <http://sedici.unlp.edu.ar/handle/10915/102488> ↑See page 92
- [Torres, 2002] Torres, A. (2002). *Probabilidad, variables aleatorias, confiabilidad y procesos estocásticos en Ingeniería Eléctrica*. Universidad de los Andes. ↑See page 93
- [Viljoen & Merwe, 2000] Viljoen, C. S., & Merwe, L. V. (2000). *Applied elementary statistics for business economics* (vol. 2). Pearson Education. ↑See page 92
- [Würfel, 2009] Würfel, P. (2009). *Physics of solar cells* (2 nd ed.). Weinheim. ↑See page 93, 95

